A Re-examination of the Synthesis of Monolayer-Protected $Co_x(SCH_2CH_2Ph)_m$ Nanoclusters: Unexpected Formation of a Thiolate-Protected Co(II) T3 Supertetrahedron

Andrew W. Cook, Guang Wu, and Trevor W. Hayton*

Department of Chemistry and Biochemistry, University of California, Santa Barbara, California 93106, United States

Supporting Information Placeholder

ABSTRACT: Herein, we report a re-examination of the synthesis and characterization of monolayer-protected $Co_x(SCH_2CH_2Ph)_m$ nanoclusters. These clusters were reportedly formed by the reaction of $CoCl_2$ with $NaBH_4$ in the presence of $HSCH_2CH_2Ph$, and were suggested to contain between 25 and 30 Co atoms. In our hands, however, we found no experimental evidence to support the existence of these large clusters in the reaction mixture. Instead, this reaction results in the relatively clean formation of the cobalt(II) coordination complex $[Co_{10}(SCH_2CH_2Ph)_{16}Cl_4]$ (**1**). Complex **1** has been fully characterized using a wide variety of techniques, including single crystal X-ray crystallography, NMR spectroscopy, mass spectrometry, and magnetometry. This complex represents the first example of a thiolate-protected Co(II) T3 supertetrahedral cluster.

Introduction

Recent advances in the synthesis of atomically-precise nanoclusters (APNCs) have resulted in a remarkable increase in the number of structurally-characterized clusters.[1-6] Despite this wealth of work, however, structurally characterized APNCs exist for only a handful of transition metal (Cu,[7-13] Ag,[5, 14-16] Au,[5, 14, 17] Pd,[18-19] and Zn[20]) and main group elements (Al,[21-24] Ga,[23, 25] Ge,[26-30] In,[31-32] and Sn[26, 28, 33-36]). Expansion to the other transition metals, such as Co, could lead to novel magnetic materials, which could have applications in catalysis, imaging, and quantum computing.[37-39] However, metallic cobalt nanomaterials are highly air-sensitive, which renders them a challenge to isolate and characterize. Several different strategies have been employed to protect these nanomaterials from unwanted oxidation, including reductive annealing to improve Co crystallinity,[40] dispersion in polymer,[41-44] coating with gold,[45-46] or embedding on a support, such as graphite[47-48] or silica.[49-50] Passivation of nanomaterials with a protective "shell" comprised of anionic and/or neutral donor ligands is another viable strategy for imparting air stability. The most common passivating ligands for APNCs are thiolates (RS^-);[2, 5] however, carbon monoxide,[18-19] hydrides[7, 9-10, 12] and acetylides[11, 13-17] have also been employed.

In 2017, Barrabés and co-workers reported the synthesis of the thiolate-protected cobalt APNCs, $Co_x(SR)_m$ (R = CH_2CH_2Ph), via reaction of $CoCl_2$ with RSH and $NaBH_4$ in THF/H_2O.[51] This material was characterized by UV-vis spectroscopy, XPS, STEM, and XANES; however, single crystals for X-ray diffraction were not forthcoming. On the basis of MALDI analysis, the authors suggested the "formation of cobalt clusters in a range of 25-30 cobalt atoms"[51] and offered $Co_{25}(SR)_{18}$ and $Co_{30}(SR)_{16}$ as two potential formulations to fit this criterion. Given the rarity of atomically-precise cobalt nanoclusters, we endeavored to reproduce the reported synthesis and further study these unique materials. Herein, we report that the major product of this reaction is actually the thiolate-protected Co(II) T3 supertetrahedron, $[Co_{10}(SR)_{16}Cl_4]$, and not a Co(0)-containing APNC, as originally reported.

Results and Discussion

The 2017 synthesis of $Co_x(SR)_m$ followed a modified Brust protocol (Scheme 1).[51-52] $CoCl_2{\cdot}6H_2O$ (1 equiv) was dehydrated at 150 °C and then dissolved in tetrahydrofuran (10 mL). $PhCH_2CH_2SH$ (3 equiv) was added to the blue solution and stirred for 30 minutes, resulting in a color change to dark blue. $NaBH_4$ (9 equiv), dissolved in H_2O (2 mL) and chilled to 0 °C, was then quickly added to the reaction mixture. The solution was stirred for 1 h and subsequently filtered and washed with methanol. The solid was then extracted with CH_2Cl_2, resulting in a pink solution containing the proposed $Co_x(SR)_m$ clusters. A yield was not reported.

Scheme 1. Original Synthetic Procedure Used to Prepare $Co_x(SCH_2CH_2Ph)_m$ Nanoclusters

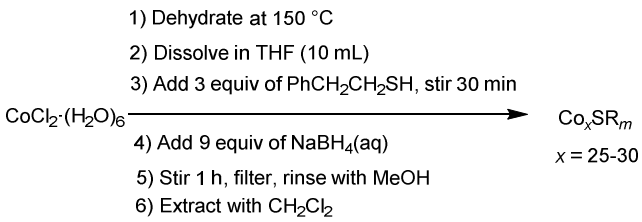

We attempted to repeat the original synthesis as closely as possible; however, we made a few minor changes to the procedure to allow for *in situ* spectroscopic monitoring. Specifically, we replaced the THF and H_2O with THF-d_8 and D_2O, respectively, and we performed the reaction in a J. Young NMR tube under an inert gas atmosphere (Figures S4 and S5). Under these conditions, we are able to successfully reproduce the deep blue solution previously reported to form upon addition of $PhCH_2CH_2SH$ to $CoCl_2$. Interestingly, upon addition of

a D_2O solution of $NaBH_4$ (9 equiv) we observe a color change to dark green. This solution then slowly turned dark brown, concomitant with the deposition of a grey-brown solid. A ^1H NMR spectrum of the reaction mixture after 30 min reveals the presence of three diagnostic resonances at -10.02, 103.22, and 120.11 ppm (Figure S4), which are assignable to the cobalt(II)-thiolate cluster, $[Co_{10}(SR)_{16}Cl_4]$ (**1**) (see below). Complex **1** is the only major product observed in the reaction mixture, demonstrating that the transformation is remarkably chemoselective.

To facilitate the isolation of **1** we repeated the above procedure in the absence of water and in an inert atmosphere glove box (Scheme 2). Work-up of this reaction mixture results in the isolation of dark brown crystals of the cobalt-thiolate cluster $[Co_{10}(SR)_{16}Cl_4]$ (**1**) in 37% yield. Also formed in this reaction is a grey-brown solid, whose appearance is consistent with that of NaCl, but which is contaminated with small amounts of a Co-containing product. We believe the modest yield of this reaction is due to the presence of excess thiol (see below), which impedes the crystallization process.

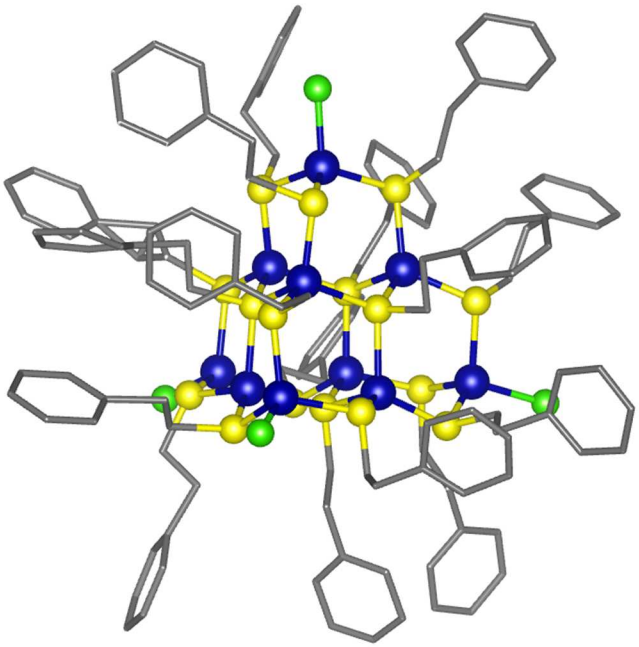

Figure 1. Ball-and-stick diagram showing **1**·2CH_2Cl_2. Hydrogen atoms and CH_2Cl_2 solvate molecules omitted for clarity. Color legend: Co = blue; S = yellow; C = grey; Cl = green

Complex **1** crystallizes in the monoclinic space group C*c* as the CH_2Cl_2 solvate, **1**·2CH_2Cl_2 (Figure 1). It features a $[Co_6S_{16}Cl_4]$ core with idealized T_d symmetry. Each of the ten Co centers features a pseudo-tetrahedral geometry and the four Cl^- ligands occupy the corners of the tetrahedron. Twelve of the 16 thiolate ligands feature a μ_2 binding mode. These are situated along the edges of the tetrahedron in six groups of two. Four of the thiolate ligands feature a μ_3 binding mode. These are situated at the centers of each triangular face. The average Co-Cl distance is 2.21 Å, which is consistent with the values reported for the related cluster, $[NBu_4]_2[Co_4(SPh)_6Cl_4]$.[53] Similarly, the Co-S distances for the μ_2 thiolate ligands (range: 2.24-2.32 Å) are within the reported range for the related Co thiolate clusters, $[NBu_4]_2[Co_4(SPh)_6Cl_4]$ and $M_2[Co_4(SPh)_{10}]$ (M = Me_4N^+, Et_4N^+,$hexyl_2NH_2^+$).[53-54] The Co-S distances for the μ_3 thiolate ligands (range: 2.30-2.35 Å) are generally longer, but overlap somewhat with those observed for the μ_2 thiolate ligands. Finally, the long Co-Co distances (range: 3.66-3.97 Å) in **1** preclude the presence of any direct Co–Co bonds. Similar Co–Co distances were also observed for $[NBu_4]_2[Co_4(SPh)_6Cl_4]$ and $M_2[Co_4(SPh)_{10}]$.[53-54]

Complex **1** is a rare example of an open-shell, chalcogenide-stabilized T3 supertetrahedral cluster.[55-56] Comparable chalcogenide-stabilized supertetrahedra, such as $[Cd_{10}(SCH_2CH_2OH)_{16}][X]_4$ (X = ClO_4^-, NO_3^-, SO_4^{2-})[57-59] and $[Me_4N]_2[E_4M_{10}(SPh)_{16}]$ (E = S, Se; M = Zn, Cd),[60] feature the diamagnetic Zn^{2+} and Cd^{2+} ions. Other open-shell supertetrahedra, such as $[M_{10}O(tmp)_4(diketonate)_4]$ (M = Ni, Co; H_3tmp = 1,1,1-tris(hydroxymethyl)propane) and $[Mn_{10}O_4(N_3)_4(hmp)_{12}][ClO_4]_2$ (Hhmp = 2-(hydroxylmethyl)pyridine) feature alkoxide co-ligands.[61-63] Complex **1** can also be viewed as the T3 analogue of known T2 supertetrahedral clusters, $M_2[Co_4(SPh)_{10}]$ (M = (Me_4N^+, Et_4N^+, $hexyl_2NH_2^+$) and $[NBu_4]_2[Co_4(SPh)_6Cl_4]$,[53-54] which are themselves closely related to the classic monometallic cobalt-thiolate complexes, $M_2[Co(SPh)_4]$ (M = PPh_4^+, Et_4N^+).[64-65]

Scheme 2. Syntheses of 1

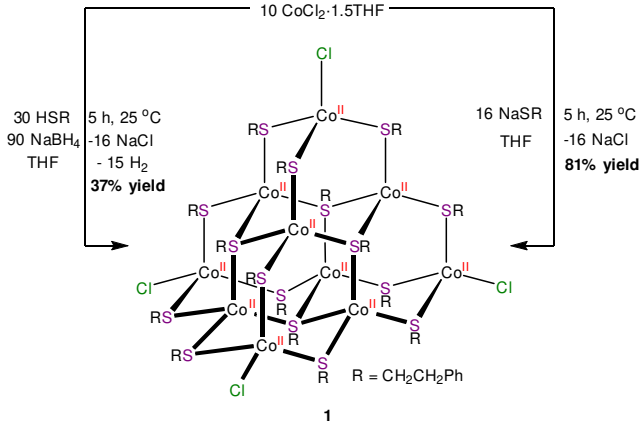

We next endeavored to synthesize complex **1** via a rational route (Scheme 2). Given that $NaBH_4$ appears to be acting solely as a base during the formation of **1**, we rationalized that the reaction protocol could be simplified by substitution of $PhCH_2CH_2SH/NaBH_4$ with $NaSCH_2CH_2Ph$. Thus, reaction of $CoCl_2$·1.5THF with 1.6 equiv of $NaSCH_2CH_2Ph$ in THF resulted in the formation of a green solution, which gradually turned dark brown over the course of 5 h, concomitant with the deposition of a grey powder. Work-up of the reaction mixture allowed for the isolation of **1** as a dark brown crystalline solid. When synthesized in this fashion complex **1** can be isolated in 81% yield.

A ^1H NMR spectrum of **1** in CD_2Cl_2 features 10 resonances, ranging from 115.7 to -19.6 ppm. The number of resonances, and their integrations, are consistent with the presence of two magnetically inequivalent thiolate environments in a 12:4 ratio, as predicted by the solid-state molecular structure. More significantly, the resonances at 115.7, 57.2, and -19.6 ppm feature very similar chemical shifts to the diagnostic resonances observed in the ^1H NMR spectrum of the *in situ* reaction mixture (see above). This further confirms that **1** is being formed in the reaction of $CoCl_2$ with $PhCH_2CH_2SH$ and $NaBH_4$ in THF/H_2O. The electrospray ionization (ESI) mass spectrum of complex **1** in CH_2Cl_2, acquired in negative ion

mode, is also consistent with our proposed formulation (Figure 2). The major feature at *m/z* = 2929.9475 is assignable to two overlapping ions: the parent peak $[M]^-$ and the fragment $[Co_9(SR)_{16}Cl_4 + Cu]^-$. Additionally, a peak at *m/z* = 2962.9119 is assignable to $[M + Cl]^-$.

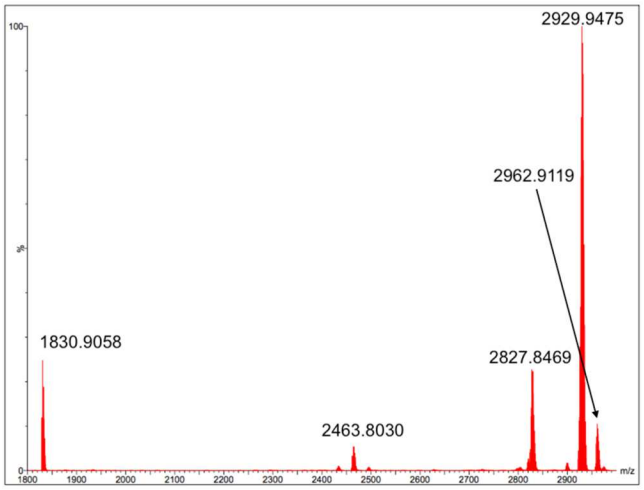

Figure 2. ESI-MS of complex **1** in negative ion mode.

Magnetic susceptibility data were also collected on a microcrystalline sample of **1** (Figure 3). At 300 K, complex **1** exhibits an effective magnetic moment of 7.36 B.M., lower than the anticipated spin-only effective magnetic moment (12.25 B.M.), and indicative of moderate antiferromagnetic coupling between cobalt centers. Dance also reported antiferromagnetic coupling between the Co centers in $[NMe_4]_2[Co_4(SPh)_{10}]$ (average J = -17 cm^{-1}).[54] Finally, the magnetization curve M vs. H is linear, implying that complex **1** is a simple paramagnet (Figure 3), and shows no hysteresis at any temperature.

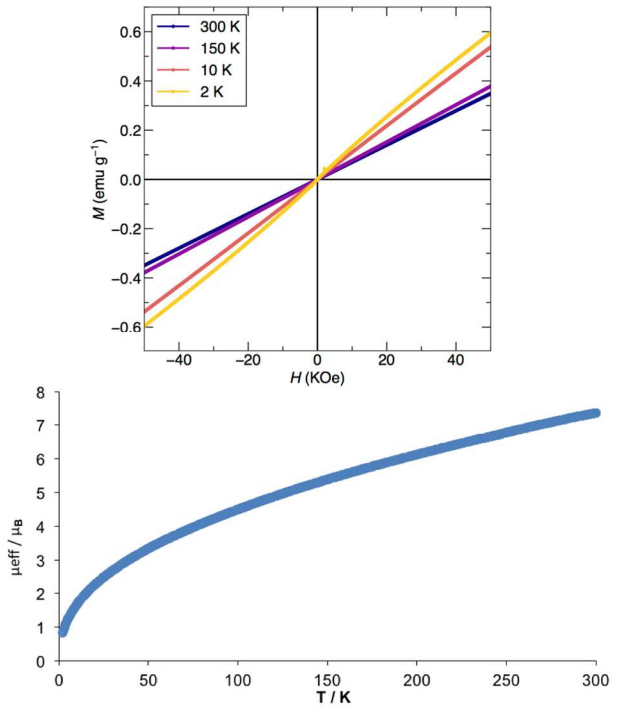

Figure 3. Solid-state magnetic susceptibility data M vs. H (top) and μ_{eff} vs. T (bottom) for **1** measured from 2 to 300 K.

We also endeavored to examine the effect of reaction stoichiometry on the formation of **1**. The reaction of $CoCl_2$·1.5THF with 1 equiv of NaSR still results in the formation of **1**, but with a significantly reduced yield (ca. 16%). Similarly, reaction of $CoCl_2$·1.5THF with 2 equiv of NaSR (Figure S7) resulted in the formation of large number of paramagnetic, Co-containing products, including complex **1** (but in insignificant amounts). Not surprisingly, we were unsuccessful in our attempts to isolate any products from this reaction mixture. From these experiments, we hypothesize that Cl^- must play an important role in directing the self-assembly of **1**. Presumably, the use of greater than 1.6 equiv of thiolate per Co results in a deficiency of Cl^-, which prevents the assembly of **1** and results in formation of a broad distribution of clusters. Previous workers have also noticed that the speciation of Co(II)-thiolates is highly dependent on reaction stoichiometry.[53-54]

We also briefly examined the chemical properties of complex **1**. It is soluble in benzene, toluene, and CH_2Cl_2, but insoluble in MeCN, Et_2O, and alkanes. Complex **1** is soluble in THF, but partially decomposes over the course of 5 h, as evidenced by the deposition of a brown solid on standing in this solvent (Figure S6). Attempted dissolution of **1** in py-d_5 results in immediate formation of a green solution that contains no resonances assignable to **1**, concomitant with deposition of a brown solid (Figure S8). While **1** clearly reacts with pyridine, we have been unable to determine the identity of the product(s) formed.

The reaction of $CoCl_2$ by $NaBH_4$, both in the presence or absence of a passivating ligand, has been studied extensively.[49-50, 66-70] In the absence of a passivating ligand, these reductions result in the formation of finely-divided Co(0) (in non-aqueous solvents) or Co_2B (under aqueous conditions).[66] In the presence of a passivating ligand, or in the presence of surfactant, the results are more complicated. In one instance, this reaction resulted in the formation of simple Co(II) thiolate complexes,[69-70] while in other cases authentic Co(0) nanoparticles were generated.[49-50, 66-68] Given this past precedent, as well as our own experiments, we believe that the 2017 synthesis initially resulted in formation of **1**, and not $Co_x(SCH_2CH_2Ph)_m$-type nanoclusters, as originally suggested. However, complex **1** then decomposed upon exposure to air and water during work-up, likely generating a mixture of $Co_xO_y(SCH_2CH_2Ph)_m$–type clusters. Consistent with this hypothesis, exposure of complex **1** to air, as a CH_2Cl_2 solution, results in a color change from deep brown to coral. A UV-vis spectrum of this solution features absorptions at 404, 493, and 611 nm (Figure S19). These values are very similar to those reported in 2017 for $Co_x(SCH_2CH_2Ph)_m$, demonstrating that the original material requires O_2 for its formation, and is therefore unlikely to contain any Co(0) character.

Conclusion

We have re-examined the synthesis of thiolate-protected cobalt APNCs by reaction of $CoCl_2$ with $NaBH_4$ and $PhCH_2CH_2SH$. Despite efforts to faithfully reproduce the reported procedure, we are unable to detect the presence of a cobalt(0)-containing APNC. Instead, we isolated the intriguing Co(II) cluster, $[Co_{10}(SR)_{16}Cl_4]$. This complex represents the first example of a thiolate-protected Co(II) T3 supertetrahedron. We believe that $[Co_{10}(SR)_{16}Cl_4]$ was also being formed in the original synthesis; however, the cluster likely reacted with oxygen and water during work-up, giving a mix of

$Co_xO_y(SCH_2CH_2Ph)_m$–type clusters. This result highlights the challenges inherent in the generation of low-valent cobalt nanoclusters, including the need for rigorous exclusion of air during their synthesis, work-up, and characterization.

ASSOCIATED CONTENT

The Supporting Information is available free of charge on the ACS Publications website.

X-ray data for compound **1**·$2CH_2Cl_2$ (CIF)

Experimental procedures, crystallographic details, and spectral data (PDF)

AUTHOR INFORMATION

Corresponding Author

*hayton@chem.ucsb.edu

Notes

The authors declare no competing financial interest.

ACKNOWLEDGMENT

We thank the National Science Foundation (CHE 1361654) for financial support. NMR spectra were collected on an instrument supported by an NIH Shared Instrumentation Grant (SIG, 1S10OD012077-01A1). ESI mass spectra were acquired at the MRL Shared Experimental Facilities, supported by the MRSEC Program of the NSF under Award No. DMR 1720256 and a member of the NSF-funded Materials Research Facilities Network. A. W. C. thanks the Mellichamp Academic Initiative in Sustainability at UCSB for a summer fellowship. We also thank Joshua Bocarsly for his assistance in the collection and interpretation of the magnetism data.

REFERENCES

1. Templeton, A. C.; Wuelfing, W. P.; Murray, R. W. Monolayer-Protected Cluster Molecules. *Acc. Chem. Res.* **2000**, *33*, 27-36.

2. Jin, R. Quantum sized, thiolate-protected gold nanoclusters. *Nanoscale* **2010**, *2*, 343-362.

3. Li, G.; Jin, R. Atomically Precise Gold Nanoclusters as New Model Catalysts. *Acc. Chem. Res.* **2013**, *46*, 1749-1758.

4. Kim, B. H.; Hackett, M. J.; Park, J.; Hyeon, T. Synthesis, Characterization, and Application of Ultrasmall Nanoparticles. *Chem. Mater.* **2014**, *26*, 59-71.

5. Jin, R.; Zeng, C.; Zhou, M.; Chen, Y. Atomically Precise Colloidal Metal Nanoclusters and Nanoparticles: Fundamentals and Opportunities. *Chem. Rev.* **2016**, *116*, 10346-10413.

6. Luo, Z.; Castleman, A. W.; Khanna, S. N. Reactivity of Metal Clusters. *Chem. Rev.* **2016**, *116*, 14456-14492.

7. Edwards, A. J.; Dhayal, R. S.; Liao, P.-K.; Liao, J.-H.; Chiang, M.-H.; Piltz, R. O.; Kahlal, S.; Saillard, J.-Y.; Liu, C. W. Chinese Puzzle Molecule: A 15 Hydride, 28 Copper Atom Nanoball. *Angew. Chem., Int. Ed.* **2014**, *53*, 7214-7218.

8. Freitag, K.; Banh, H.; Gemel, C.; Seidel, R. W.; Kahlal, S.; Saillard, J.-Y.; Fischer, R. A. Molecular brass: Cu_4Zn_4, a ligand protected superatom cluster. *Chem. Commun.* **2014**, *50*, 8681-8684.

9. Ganesamoorthy, C.; Weßing, J.; Kroll, C.; Seidel, R. W.; Gemel, C.; Fischer, R. A. The Intermetalloid Cluster $[(Cp^*AlCu)_6H_4]$, Embedding a Cu_6 Core Inside an Octahedral Al_6 Shell: Molecular Models of Hume–Rothery Nanophases. *Angew. Chem., Int. Ed.* **2014**, *53*, 7943-7947.

10. Nguyen, T.-A. D.; Jones, Z. R.; Goldsmith, B. R.; Buratto, W. R.; Wu, G.; Scott, S. L.; Hayton, T. W. A Cu_{25} Nanocluster with Partial Cu(0) Character. *J. Am. Chem. Soc.* **2015**, *137*, 13319-13324.

11. Chakrahari, K. K.; Liao, J.-H.; Kahlal, S.; Liu, Y.-C.; Chiang, M.-H.; Saillard, J.-Y.; Liu, C. W. $[Cu_{13}\{S_2CN^nBu_2\}_6(acetylide)_4]^+$: A Two-Electron Superatom. *Angew. Chem., Int. Ed.* **2016**, *55*, 14704-14708.

12. Nguyen, T.-A. D.; Jones, Z. R.; Leto, D. F.; Wu, G.; Scott, S. L.; Hayton, T. W. Ligand-Exchange-Induced Growth of an Atomically Precise Cu_{29} Nanocluster from a Smaller Cluster. *Chem. Mater.* **2016**, *28*, 8385-8390.

13. Cook, A. W.; Jones, Z. R.; Wu, G.; Scott, S. L.; Hayton, T. W. An Organometallic Cu_{20} Nanocluster: Synthesis, Characterization, Immobilization on Silica, and "Click" Chemistry. *J. Am. Chem. Soc.* **2018**, *140*, 394-400.

14. Lei, Z.; Wan, X.-K.; Yuan, S.-F.; Wang, J.-Q.; Wang, Q.-M. Alkynyl-protected gold and gold-silver nanoclusters. *Dalton Trans.* **2017**, *46*, 3427-3434.

15. Qu, M.; Li, H.; Xie, L.-H.; Yan, S.-T.; Li, J.-R.; Wang, J.-H.; Wei, C.-Y.; Wu, Y.-W.; Zhang, X.-M. Bidentate Phosphine-Assisted Synthesis of an All-Alkynyl-Protected Ag_{74} Nanocluster. *J. Am. Chem. Soc.* **2017**, 12346-12349.

16. Yuan, S.-F.; Li, P.; Tang, Q.; Wan, X.-K.; Nan, Z.-A.; Jiang, D.-e.; Wang, Q.-M. Alkynyl-protected silver nanoclusters featuring an anticuboctahedral kernel. *Nanoscale* **2017**, 11405-11409.

17. Wan, X.-K.; Cheng, X.-L.; Tang, Q.; Han, Y.-Z.; Hu, G.; Jiang, D.-e.; Wang, Q.-M. Atomically Precise Bimetallic $Au_{19}Cu_{30}$ Nanocluster with an Icosidodecahedral Cu_{30} Shell and an Alkynyl–Cu Interface. *J. Am. Chem. Soc.* **2017**, 9451-9454.

18. Mednikov, E. G.; Jewell, M. C.; Dahl, L. F. Nanosized $(\mu_{12}\text{-}Pt)Pd_{164-x}Pt_x(CO)_{72}(PPh_3)_{20}$ ($x \approx 7$) Containing Pt-Centered Four-Shell 165-Atom Pd–Pt Core with Unprecedented Intershell Bridging Carbonyl Ligands: Comparative Analysis of Icosahedral Shell-Growth Patterns with Geometrically Related $Pd_{145}(CO)_x(PEt_3)_{30}$ ($x \approx 60$) Containing Capped Three-Shell Pd_{145} Core. *J. Am. Chem. Soc.* **2007**, *129*, 11619-11630.

19. Erickson, J. D.; Mednikov, E. G.; Ivanov, S. A.; Dahl, L. F. Isolation and Structural Characterization of a Mackay 55-Metal-Atom Two-Shell Icosahedron of Pseudo-I_h Symmetry, $Pd_{55}L_{12}(\mu_3\text{-}CO)_{20}$ (L = PR_3, R = Isopropyl): Comparative Analysis with Interior Two-Shell Icosahedral Geometries in Capped Three-Shell Pd_{145}, Pt-Centered Four-Shell Pd–Pt M_{165}, and Four-Shell Au_{133} Nanoclusters. *J. Am. Chem. Soc.* **2016**, *138*, 1502-1505.

20. Banh, H.; Dilchert, K.; Schulz, C.; Gemel, C.; Seidel, R. W.; Gautier, R.; Kahlal, S.; Saillard, J. Y.; Fischer, R. A. Atom-Precise Organometallic Zinc Clusters. *Angew. Chem., Int. Ed.* **2016**, *55*, 3285-3289.

21. Ecker, A.; Weckert, E.; Schnöckel, H. Synthesis and structural characterization of an Al_{77} cluster. *Nature* **1997**, *387*, 379-381.

22. Huber, M.; Schnepf, A.; Anson, C. E.; Schnöckel, H. $Si@Al_{56}[N(2,6\text{-}{}^iPr_2C_6H_3)SiMe_3]_{12}$: The Largest Neutral Metalloid Aluminum Cluster, a Molecular Model for a Silicon-Poor Aluminum–Silicon Alloy? *Angew. Chem., Int. Ed.* **2008**, *47*, 8201-8206.

23. Schnöckel, H. Formation, structure and bonding of metalloid Al and Ga clusters. A challenge for chemical efforts in nanosciences. *Dalton Trans.* **2008**, 4344-4362.

24. Henke, P.; Trapp, N.; Anson, C. E.; Schnöckel, H. $Al_{12}K_8[OC(CH_3)_3]_{18}$: A Wade, Zintl, or Metalloid Cluster, or a Hybrid of All Three? *Angew. Chem., Int. Ed.* **2010**, *49*, 3146-3150.

25. Wolf, R.; Uhl, W. Main-Group-Metal Clusters Stabilized by N-Heterocyclic Carbenes. *Angew. Chem., Int. Ed.* **2009**, *48*, 6774-6776.

26. Schnepf, A. Metalloid group 14 cluster compounds: An introduction and perspectives to this novel group of cluster compounds. *Chem. Soc. Rev.* **2007**, *36*, 745-758.

27. Schenk, C.; Schnepf, A. $Ge_{14}[Ge(SiMe_3)_3]_5Li_3(THF)_6$: the largest metalloid cluster compound of germanium: on the way to fullerene-like compounds? *Chem. Commun.* **2008**, 4643-4645.

28. Scharfe, S.; Kraus, F.; Stegmaier, S.; Schier, A.; Fässler, T. F. Zintl Ions, Cage Compounds, and Intermetalloid Clusters of Group 14 and Group 15 Elements. *Angew. Chem., Int. Ed.* **2011**, *50*, 3630-3670.

29. Schenk, C.; Kracke, A.; Fink, K.; Kubas, A.; Klopper, W.; Neumaier, M.; Schnöckel, H.; Schnepf, A. The Formal Combination of Three Singlet Biradicaloid Entities to a Singlet Hexaradicaloid Metalloid $Ge_{14}[Si(SiMe_3)_3]_5[Li(THF)_2]_3$ Cluster. *J. Am. Chem. Soc.* **2011**, *133*, 2518-2524.

30. Kysliak, O.; Schrenk, C.; Schnepf, A. The Largest Metalloid Group 14 Cluster, $Ge_{18}[Si(SiMe_3)_3]_6$: An Intermediate on the Way to Elemental Germanium. *Angew. Chem., Int. Ed.* **2016**, *55*, 3216-3219.

31. Protchenko, A. V.; Dange, D.; Blake, M. P.; Schwarz, A. D.; Jones, C.; Mountford, P.; Aldridge, S. Oxidative Bond Formation and Reductive Bond Cleavage at Main Group Metal Centers: Reactivity of Five-Valence-Electron MX_2 Radicals. *J. Am. Chem. Soc.* **2014**, *136*, 10902-10905.

32. Aldridge, S.; Protchenko, A.; Urbano, J.; Abdalla, J.; Campos, J.; Vidovic, D.; Schwarz, A.; Blake, M.; Mountford, P.; Jones, C. Electronic Delocalization in Two and Three Dimensions: Differential Aggregation in Indium 'Metalloid' Clusters. *Angew. Chem., Int. Ed.* **2017**, 15098-15102.

33. Brynda, M.; Herber, R.; Hitchcock, P. B.; Lappert, M. F.; Nowik, I.; Power, P. P.; Protchenko, A. V.; Růžička, A.; Steiner, J. Higher-Nuclearity Group 14 Metalloid Clusters: $[Sn_9\{Sn(NRR')\}_6]$. *Angew. Chem., Int. Ed.* **2006**, *45*, 4333-4337.

34. Schrenk, C.; Winter, F.; Pöttgen, R.; Schnepf, A. $\{Sn_9[Si(SiMe_3)_3]_2\}^{2-}$: A Metalloid Tin Cluster Compound With a Sn_9 Core of Oxidation State Zero. *Inorg. Chem.* **2012**, *51*, 8583-8588.

35. Schrenk, C.; Winter, F.; Pöttgen, R.; Schnepf, A. $\{Sn_{10}[Si(SiMe_3)_3]_4\}^{2-}$: A Highly Reactive Metalloid Tin Cluster with an Open Ligand Shell. *Chem. – Eur. J.* **2015**, *21*, 2992-2997.

36. Wiederkehr, J.; Wolper, C.; Schulz, S. Synthesis and solid state structure of a metalloid tin cluster $[Sn_{10}(trip_8)]$. *Chem. Commun.* **2016**, *52*, 12282-12285.

37. Schätz, A.; Reiser, O.; Stark, W. J. Nanoparticles as Semi-Heterogeneous Catalyst Supports. *Chem. – Eur. J.* **2010**, *16*, 8950-8967.

38. Colombo, M.; Carregal-Romero, S.; Casula, M. F.; Gutierrez, L.; Morales, M. P.; Bohm, I. B.; Heverhagen, J. T.; Prosperi, D.; Parak, W. J. Biological applications of magnetic nanoparticles. *Chem. Soc. Rev.* **2012**, *41*, 4306-4334.

39. Tejada, J.; Chudnovsky, E. M.; del Barco, E.; Hernandez, J. M.; Spiller, T. P. Magnetic qubits as hardware for quantum computers. *Nanotechnology* **2001**, *12*, 181.

40. Wu, L.; Li, Q.; Wu, C. H.; Zhu, H.; Mendoza-Garcia, A.; Shen, B.; Guo, J.; Sun, S. Stable Cobalt Nanoparticles and Their Monolayer Array as an Efficient Electrocatalyst for Oxygen Evolution Reaction. *J. Am. Chem. Soc.* **2015**, *137*, 7071-7074.

41. Osuna, J.; de Caro, D.; Amiens, C.; Chaudret, B.; Snoeck, E.; Respaud, M.; Broto, J.-M.; Fert, A. Synthesis, Characterization, and Magnetic Properties of Cobalt Nanoparticles from an Organometallic Precursor. *J. Chem. Phys.* **1996**, *100*, 14571-14574.

42. Verelst, M.; Ely, T. O.; Amiens, C.; Snoeck, E.; Lecante, P.; Mosset, A.; Respaud, M.; Broto, J. M.; Chaudret, B. Synthesis and Characterization of CoO, Co_3O_4, and Mixed Co/CoO Nanoparticules. *Chem. Mater.* **1999**, *11*, 2702-2708.

43. Puntes, V. F.; Krishnan, K. M.; Alivisatos, A. P. Colloidal Nanocrystal Shape and Size Control: The Case of Cobalt. *Science* **2001**, *291*, 2115-2117.

44. Keng, P. Y.; Shim, I.; Korth, B. D.; Douglas, J. F.; Pyun, J. Synthesis and Self-Assembly of Polymer-Coated Ferromagnetic Nanoparticles. *ACS Nano* **2007**, *1*, 279-292.

45. Bao, Y.; Calderon, H.; Krishnan, K. M. Synthesis and Characterization of Magnetic-Optical Co–Au Core–Shell Nanoparticles. *J. Phys. Chem. C* **2007**, *111*, 1941-1944.

46. Song, Y.; Ding, J.; Wang, Y. Shell-Dependent Evolution of Optical and Magnetic Properties of Co@Au Core–Shell Nanoparticles. *J. Phys. Chem. C* **2012**, *116*, 11343-11350.

47. Lu, A.-H.; Li, W.-C.; Matoussevitch, N.; Spliethoff, B.; Bonnemann, H.; Schuth, F. Highly stable carbon-protected cobalt nanoparticles and graphite shells. *Chem. Commun.* **2005**, 98-100.

48. Grass, R. N.; Athanassiou, E. K.; Stark, W. J. Covalently Functionalized Cobalt Nanoparticles as a Platform for Magnetic Separations in Organic Synthesis. *Angew. Chem., Int. Ed.* **2007**, *46*, 4909-4912.

49. Kobayashi, Y.; Horie, M.; Konno, M.; Rodríguez-González, B.; Liz-Marzán, L. M. Preparation and Properties of Silica-Coated Cobalt Nanoparticles. *J. Phys. Chem. B* **2003**, *107*, 7420-7425.

50. Salgueirino-Maceira, V.; Correa-Duarte, M. A. Cobalt and silica based core-shell structured nanospheres. *J. Mater. Chem.* **2006**, *16*, 3593-3597.

51. Pollitt, S.; Pittenauer, E.; Rameshan, C.; Schachinger, T.; Safonova, O. V.; Truttmann, V.; Bera, A.; Allmaier, G.; Barrabés, N.; Rupprechter, G. Synthesis and Properties of Monolayer-Protected $Co_x(SC_2H_4Ph)_m$ Nanoclusters. *J. Phys. Chem. C* **2017**, *121*, 10948-10956.

52. Goulet, P. J. G.; Lennox, R. B. New Insights into Brust–Schiffrin Metal Nanoparticle Synthesis. *J. Am. Chem. Soc.* **2010**, *132*, 9582-9584.

53. Fenske, D.; Meyer, J.; Merzweiler, K. Zur Reaktion von $PhSSiMe_3$ mit $[CoCl_2(PPh_3)_2]$ und $(NBu_4)[CoCl_3(PPh_3)]$. Die Kristallstrukturen von $(NBu_4)_2[Co_4(SPh)_6Cl_4]$, $[Co_4(SPh)_6Cl_2(POPh_3)(PPh_3)]$ und $(NBu_4)[Mn_2(SPh)_3(CO)_6]$. *Z. Naturforsch* **1987**, *42b*, 1207–1211.

54. Dance, I. G. Synthesis, Crystal Structure, and Properties of the Hexa(μ-benzenethiolato)tetra(benzenethiolatocobaltate(II)) Dianion, the Prototype Cobalt(II)-Thiolate Molecular Cluster. *J. Am. Chem. Soc.* **1979**, *101*, 6264-6273.

55. Feng, P.; Bu, X.; Zheng, N. The Interface Chemistry between Chalcogenide Clusters and Open Framework Chalcogenides. *Acc. Chem. Res.* **2005**, *38*, 293-303.

56. Levchenko, T. I.; Huang, Y.; Corrigan, J. F., Large Metal Chalcogenide Clusters and Their Ordered Superstructures via Solvothermal and Ionothermal Syntheses. In *Clusters – Contemporary Insight in Structure and Bonding*, Dehnen, S., Ed. Springer International Publishing: Cham, 2017; pp 269-319.

57. Strickler, P. The Structure of a Novel Polynuclear Complex related to the Sphalerite Lattice. *J. Chem. Soc. D* **1969**, 655b-656.

58. Bürgi, H.-B. Stereochemistry of Polynuclear Cadmium(II) Thioglycolates: Crystal structure of cadmium(II) bisthioglycolate. *Helv. Chim. Acta* **1974**, *57*, 513-519.

59. Lacelle, S.; Stevens, W. C.; Kurtz, D. M.; Richardson, J. W.; Jacobson, R. A. Crystal and Molecular Structure of $[Cd_{10}(SCH_2CH_2OH)_{16}](ClO_4)_4{\cdot}8H_2O$. Correlations with Cadmium-113 NMR Spectra of the Solid and Implications for Cadmium-Thiolate Ligation in Proteins. *Inorg. Chem.* **1984**, *23*, 930-935.

60. Dance, I. G.; Choy, A.; Scudder, M. L. Syntheses, Properties, and Molecular and Crystal Structures of $(Me_2N)_4[E_4M_{10}(SPh)_{16}]$ (E = Sulfur or Selenium; M = Zinc or Cadmium): Molecular Supertetrahedral Fragments of the Cubic Metal Chalcogenide Lattice. *J. Am. Chem. Soc.* **1984**, *106*, 6285-6295.

61. Lisnard, L.; Tuna, F.; Candini, A.; Affronte, M.; Winpenny, R. E. P.; McInnes, E. J. L. Supertetrahedral and Bi-supertetrahedral Cages: Synthesis, Structures, and Magnetic Properties of Deca- and Enneadecametallic Cobalt(II) Clusters. *Angew. Chem., Int. Ed.* **2008**, *47*, 9695-9699.

62. Shaw, R.; Tidmarsh, I. S.; Laye, R. H.; Breeze, B.; Helliwell, M.; Brechin, E. K.; Heath, S. L.; Murrie, M.; Ochsenbein, S.; Gudel, H.-U.; McInnes, E. J. L. Supertetrahedral decametallic Ni(II) clusters directed by μ_6-*tris*-alkoxides. *Chem. Commun.* **2004**, 1418-1419.

63. Stamatatos, T. C.; Abboud, K. A.; Wernsdorfer, W.; Christou, G. Ferromagnetically-coupled decanuclear, mixed-valence $[Mn_{10}O_4(N_3)_4(hmp)_{12}]^{2+}$ [hmpH = 2-(hydroxymethyl)pyridine] clusters with rare *T* symmetry and an *S* = 22 ground state. *Polyhedron* **2007**, *26*, 2042-2046.

64. Swenson, D.; Baenziger, N. C.; Coucouvanis, D. Tetrahedral Mercaptide Complexes. Crystal and Molecular Structures of $[(C_6H_5)_4P]_2M(SC_6H_5)_4$ Complexes (M = Cadmium(II), Zinc(II), Nickel(II), Cobalt(II), and Manganese(II)). *J. Am. Chem. Soc.* **1978**, *100*, 1932-1934.

65. Suturina, E. A.; Nehrkorn, J.; Zadrozny, J. M.; Liu, J.; Atanasov, M.; Weyhermüller, T.; Maganas, D.; Hill, S.; Schnegg, A.; Bill, E.; Long, J. R.; Neese, F. Magneto-Structural Correlations in Pseudotetrahedral Forms of the $[Co(SPh)_4]^{2-}$ Complex Probed by Magnetometry, MCD Spectroscopy, Advanced EPR Techniques, and ab Initio Electronic Structure Calculations. *Inorg. Chem.* **2017**, *56*, 3102-3118.

66. Glavee, G. N.; Klabunde, K. J.; Sorensen, C. M.; Hadjipanayis, G. C. Sodium Borohydride Reduction of Cobalt Ions in Nonaqueous

Media. Formation of Ultrafine Particles (Nanoscale) of Cobalt Metal. *Inorg. Chem.* **1993**, *32*, 474-477.

67. Lin, X. M.; Sorensen, C. M.; Klabunde, K. J.; Hadjipanayis, G. C. Temperature Dependence of Morphology and Magnetic Properties of Cobalt Nanoparticles Prepared by an Inverse Micelle Technique. *Langmuir* **1998**, *14*, 7140-7146.

68. Salgueiriño-Maceira, V.; Correa-Duarte, M. A.; Farle, M.; López-Quintela, M. A.; Sieradzki, K.; Diaz, R. Synthesis and Characterization of Large Colloidal Cobalt Particles. *Langmuir* **2006**, *22*, 1455-1458.

69. Sanghamitra, N. J. M.; Mazumdar, S. Effect of Polar Solvents on the Optical Properties of Water-Dispersible Thiol-Capped Cobalt Nanoparticles. *Langmuir* **2008**, *24*, 3439-3445.

70. Kitaev, V. Comment on Effect of Polar Solvents on the Optical Properties of Water-Dispersible Thiol-Capped Cobalt Nanoparticles. *Langmuir* **2008**, *24*, 7623-7624.

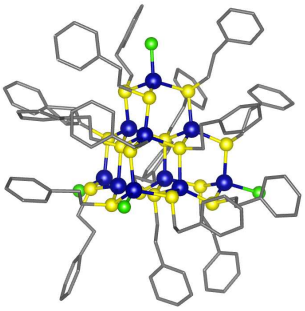

Reaction of $CoCl_2$ with $NaBH_4$ and $HSCH_2CH_2Ph$, in THF, results in formation of $[Co_{10}(SCH_2CH_2Ph)_{16}Cl_4]$. This complex represents the first example of a thiolate-protected Co(II) T3 supertetrahedron.